Hybrid ISMC-PIO and Receding Horizon Control for UAVs Formation

Xiaobin Xu
School of Automation Science and Electrical Engineering
Beihang University(BUAA)
Beijing, China
xiaobinxu@buaa.edu.cn

Haibin Duan, *Senior Member, IEEE*
1. *Beihang University(BUAA)*
Beijing, China
2. *Pengcheng Laboratory*
Shenzhen, China
hbduan@buaa.edu.cn

Yimin Deng
School of Automation Science and Electrical Engineering
Beihang University(BUAA)
Beijing, China
ymdeng@buaa.edu.cn

Delin Luo
School of Aerospace Engineering
Xiamen University
Xiamen, China
luodelin1204@xmu.edu.cn

***Abstract*—Unmanned aerial vehicles (UAVs) formation can achieve considerable missions. Control strategy plays an important role in UAVs formation. In this paper, a receding horizon control (RHC) for UAVs formation based on independent search and multi-area convergence pigeon-inspired optimization (ISMC-PIO) is proposed. To minimize the cost value for measuring UAVs formation process, the modified pigeon-inspired optimization (PIO) is utilized by converting the RHC parameters and performance index for UAVs formation problem to a global optimization problem. PIO is a novel bio-inspired algorithm. However, basic PIO has the disadvantages of slower convergence speed and falling into local optimum easily. The modified PIO has faster convergence rate and global search ability by importing independent search factor and multi-area convergence strategy. Numerous experiments are implemented to prove that the ISMC-PIO can converge quickly and obtain a better cost value.**

Keywords—independent search and multi-area convergence (IS MC), pigeon-inspired optimization (PIO), receding horizon control (RHC), unmanned aerial vehicle (UAV)

I. INTRODUCTION

Unmanned aerial vehicles (UAVs) are characterized by low cast, simple equipment, flexibility and unmanned casualties [1]. UAVs are widely employed in military and civil, such as cooperative reconnaissance, defense and pesticide spraying etc. UAVs formation is an organization mode with two or more UAVs [2]. They are arranged in a specific formation to meet the mission. The resources of each UAV in the formation would be shared. The success rate and ability of resisting emergencies are improved [3]. UAVs formation is an inevitable trend for perform dangerous missions [4]. Therefore, UAVs formation flight is a technology pursued by military and scientific researchers all over the word.

UAVs formation control is an important technology of multi-UAV cooperative control technology [5]. Sliding mode control method is used to design the formation controller by Ghamry Team [6]. Kim et al. proposed a distributed behavior controller based on feedback linearization method for UAVs formation [7]. PID controller with Kalman filter is employed for UAVs formation by Zhang et al. [8]. A distributed controller based on behavior method is implemented by Shin et al. It has the aid of state information of adjacent UAVs [9]. Li et al. presented a synchronization controller for UAVs autonomous formation [10]. UAVs formation control based on behavior and virtual structure is applied by Cai et al.[11].

Receding horizon control (RHC) is an effective predictive control technology. It is used to solve the optimization control problems by the current state of the system constantly [12]. UAVs formation is a strong coupling and comprehensiveness online computing optimization process. Performance of UAVs formation can be evaluated by the cost function with RHC. The parameters of RHC for formation are more and complicated. The optimization algorithms shows superiority in solving the parameter optimization problem, such as particle swarm (PSO) [13], genetic algorithm [14], artificial bee colony (ABC) [15], brain storm optimization (BSO) [16] etc. Bio-inspired algorithms are known as robustness, adaptability etc. They are suitable for RHC parameters optimization for UAVs formation.

Pigeon-inspired optimization (PIO) is an amusing swarm intelligent optimization algorithm [17]. PIO imitates the homing behavior of pigeons. The sun, compass and landmark are regarded as navigation tools in different stages of homing. However, PIO has shortcoming of falling into local optimum easily and converging slowly. To improve the performance of RHC for UAVs formation, a novel PIO is implemented. The independent search and multi-area convergence mechanisms are employed to modify the property of the basic PIO.

The organizational structure of the rest parts is as follow. The basic PIO and the proposed ISMC-PIO are introduced in Session II. Session III provides the model of UAVs and RHC for UAVs formation. A plurality of experimental results are presented in Session IV. Session V gives the conclusions.

II. INDEPENDENT SEARCH AND MULTI-AREA CONVERGENCE PIGEON-INSPIRED OPTIMIZATION

A. Pigeon-Inspired Optimization

Pigeons are renowned for their remarkable navigation abilities. The homing behavior of pigeons is affected by three main factors, the sun, the earth magnetic and the landmark [17]. They are transformed to three mathematical models, the map operator, the compass operator and the landmark operator respectively. And they are applied in different stages of the

The work was supported by the National Natural Science Foundation of China under #61803011, #61425008, and #91648205.

honing journey. Two independent simulation phases are used to imitate the homing behavior. At the beginning, pigeons rely on the map operator and compass operator in the most time. Then, the landmark operator is employed when pigeons arrive near their destination. In this process, pigeons adjust their flight status based on the pigeons who are familiar with the environment near the destination.

Firstly, pigeons rely on the map and compass operator. And they fly to the destination in a rough direction. Suppose that N is the number of pigeons. $\boldsymbol{X}_i = [x_{i1}, x_{i2}, x_{i3} \cdots, x_{iD}]$ and $\boldsymbol{V}_i = [v_{i1}, v_{i2}, v_{i3}, \cdots, v_{iD}]$ are the position and the velocity of pigeons i respectively, where D is the dimension of position and velocity, and $i = 1, 2, 3, \cdots, N$. T_1 is the number of iteration of the map and compass stage. Therefore, the map and compass operator is given by

$$\begin{cases} \boldsymbol{V}_i^t = V_i^{t-1} \cdot e^{-R*t} + rand \cdot (X_{gbest} - X_i^{t-1}) \\ \boldsymbol{X}_i^t = X_i^{t-1} + V_i^t \end{cases} \quad (1)$$

where $\boldsymbol{X}_i^t$ is the current position of pigeon i at t_th generation, the current generation is said by t, $\boldsymbol{V}_i^t$ denotes the current velocity of pigeon i at t_th generation, the map and compass factor is said by R, $rand$ represents a random value among 0 to 1, the best location of all pigeons is expressed by $\boldsymbol{X}_{gbest}$.

Secondly, pigeons are getting closing to their destination. In this stage, the landmark operator is regarded as the main navigation tool rather than the map and compass. The number of generation of this stage is T_2. The flight rules of this pigeons is expressed by

$$\begin{cases} N^t = N^{t-1}/2 \\ \boldsymbol{X}_{center}^{t-1} = \sum_{i=1}^{N^{t-1}} \boldsymbol{X}_i^{t-1} \cdot f_{cost}(\boldsymbol{X}_i^{t-1}) \Big/ (N^{t-1} \cdot \sum_{i=1}^{N^{t-1}} f_{cost}(\boldsymbol{X}_i^{t-1})) \\ \boldsymbol{X}_i^t = \boldsymbol{X}_i^{t-1} + rand \cdot (\boldsymbol{X}_{center}^{t-1} + \boldsymbol{X}_i^{t-1}) \end{cases} \quad (2)$$

In the second phase, half of pigeons N^t with better flight condition are selected in every generation. The center of these selected pigeons $\boldsymbol{X}_{center}^{t-1}$ is voted. This pigeon, who is familiar with the landmark near the destination, is followed by others. $f_{cost}(\boldsymbol{X}_i^{t-1})$ is fitness value of $\boldsymbol{X}_i$ at t_th generation. Similarly, $rand$ is a random value among 0 to 1.

B. Independent Search and Multi-area Convergence Pigeon-inspired Optimization

The basic PIO optimization algorithm is efficient to some optimization problems. However, falling into local optimum solution is a fatal flaw. Therefore, the independent search mechanism is employed in the improved algorithm. It could avoid falling into the local optimum. In addition, multi-areas, which contain suspicious optimum solution, would be searched comprehensively. This strategy is helpful to improve the accuracy. Similarly, the improved independent search and multi-area convergence pigeon-inspired optimization (ISMC-PIO) is divided into two standalone stages.

In the "map and compass navigation" stage, the global optimum is used merely to update the velocity and position of every pigeon. To enhance the global search capability and avoid to fall in to the local optimum, the local optimum and the global optimum are both employed in this part. The diagram of the independent search strategy is shown in Fig.1.

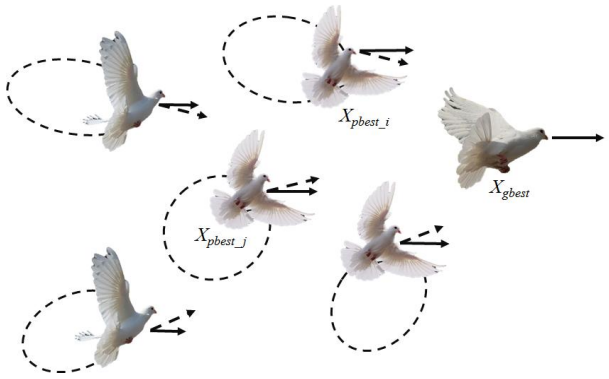

Fig. 1. The diagram of the independent search mechanism.

As shown in Fig.1, the update rules of velocity and position are shown by

$$\begin{cases} \boldsymbol{V}_i^t = \boldsymbol{V}_i^{t-1} \cdot e^{-R \cdot t} + c \cdot (r_1 \cdot (\boldsymbol{X}_{gbest} - \boldsymbol{X}_i^{t-1}) + r_2 \cdot (\boldsymbol{X}_{pbest\_i}^{t-1} - \boldsymbol{X}_i^{t-1})) \\ \boldsymbol{X}_i^t = \boldsymbol{X}_i^{t-1} + \boldsymbol{V}_i^t \end{cases} \quad (3)$$

where $\boldsymbol{X}_{pbest\_i}^t$ expresses the local optimum value of pigeon i, r_1, r_2 are two random value among 0 to 1, the local optimum value of pigeon i at t_th generation is expressed by $\boldsymbol{X}_{pbest\_i}^{t-1}$, c is the learning factor. After considerable contrast calculations experience, c is defined to 2.

In the "landmark" stage, half of all pigeons are employed to search the global optimum. Multi-area convergence mechanism is used to search the non-inferior solutions. Non-inferior solution is a suspicious optimum solution. The fitness value of it is close to the searched optimal pigeon. The definition of the non-inferior solutions is given by

$$\left| f_{cost}(\boldsymbol{X}_i^t) - f_{cost}(\boldsymbol{X}_{gbest}) \right| < \lambda \cdot \left| f_{cost}^{average}(\boldsymbol{X}) - f_{cost}(\boldsymbol{X}_{gbest}) \right| \quad (4)$$

where $f_{cost}^{average}(\boldsymbol{X})$ is an average of all pigeons' local optimum fitness so far, the coordination parameter is said by λ. Searching non-inferior solutions can avoid falling into the local. However, the number of non-inferior solutions influence the search accuracy. The coordination parameter can adjust the number of non-inferior solutions. The search accuracy can be

improved by reducing the number of non-inferior solutions. The coordination parameter is given by

$$\lambda = \log_{1/2} - t/T \tag{5}$$

where t is the current generation, $T = T_1 + T_2$ expresses the total iteration.

Therefore, when the position of pigeon i is a non-inferior solution, the renewal mechanism in the landmark stage is shown by

$$\boldsymbol{X}_i^t = \boldsymbol{X}_{pbest\_i}^{t-1} + \eta \cdot e^{(t-1)/T} \cdot (\boldsymbol{X}_{upper} - \boldsymbol{X}_{lower})/\gamma \tag{6}$$

where $\eta = [\eta_1, \eta_2, \cdots \eta_i \cdots \eta_D], i = 1, 2, \cdots \mathrm{D}$, η_i is random value among -1 to1, γ is defined as 20, $\boldsymbol{X}_{upper}$ and $\boldsymbol{X}_{lower}$ donate the upper and lower limit of searching space respectively. Otherwise, the update rule is the same as the third of (2).

The diagram of the multi-area convergence mechanism is shown in Fig.2. On the one hand, the global optimum pigeon is followed by a part of pigeons. On the other hand, the neighborhood of the non-inferior solutions would be searched. Some pigeons move in this neighborhood rather than the searched global optimum solution.

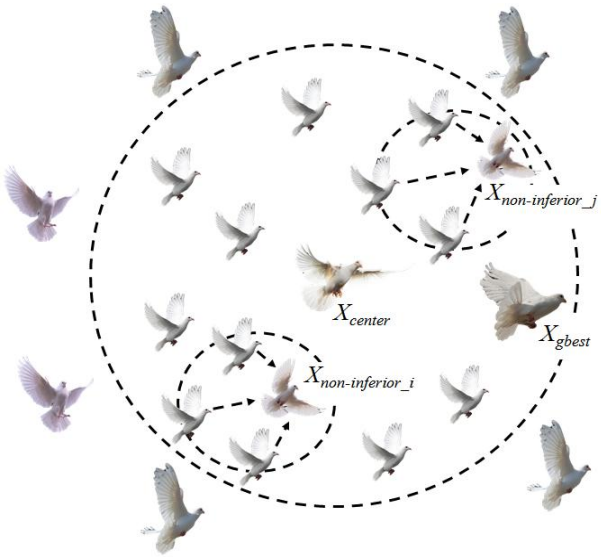

Fig. 2. The diagram of the multi-area convergence mechanism.

The ISMC-PIO algorithm is employed to optimize the parameters of the nonlinear RHC model of UAVs. Then, the most appropriate controller parameters is applied for the UAVs formation. The implementation steps of ISMC-PIO is described.

- *Step1*: Initialize the parameters of ISMC-PIO, such as *N* (the whole number of pigeons), *D* (the dimension of each pigeon), $\boldsymbol{X}^0$ and $\boldsymbol{V}^0$ (the initial position and velocity), *R* (the map and compass index), *c* (the learning factor), etc.
- *Step2*: Update the position $\boldsymbol{X}_i$ and velocity $\boldsymbol{V}_i$ of every pigeon and calculate the fitness value $f_{\cos t}$ of each one according to (3).
- *Step3*: Update the local optimum $\boldsymbol{X}_{pbest\_i}$ of pigeon i and the global optimum $\boldsymbol{X}_{gbest}$ of all pigeon until the current generation.
- *Step4*: Execute Step 2 while $t < T_1$. Otherwise return *Step 5*.
- *Step 5*: Half of pigeons are selected to implement the landmark operator. Obtain the center position $\boldsymbol{X}_{center}$ of all pigeons and get the fitness value of them according to (2).
- *Step 6*: If $\boldsymbol{X}_i$ is a non-inferior solution based on (4), $\boldsymbol{X}_i$ is updated by (6), or else by the third of (2).
- *Step 7*: Evaluate the fitness value $f_{\cos t}$.
- *Step 8*: Execute Step 5 while $t < T_2$. Otherwise achieve the global optimum.

C. Complexity Analysis on PIO and ISMC-PIO

Time complexity is an important index to measure the efficiency of algorithm. The basic PIO consists of two major parts, the map and compass stage and the landmark stage. In the first stage, the time complexity is expressed by $O((f_{\cos t} + D) \cdot N^t)$ based on (1) in each generation. In the second stage, the time complexity is calculated by $O(N^t \cdot \log N^t + D \cdot \log N^t + f_{\cos t} \cdot \log N^t)$ because of (2) in every iteration. In conclusion, the time complexity of the basic PIO is $O(N'(N^t \cdot \log N^t + D \cdot N^t + f_{\cos t} \cdot N^t))$, where N' is the all generations.

Similarly, the improved ISMC-PIO is also divided into the map and compass phase and the landmark phase. Distinguish from PIO, the local optimum solution and the non-inferior solutions are leaded into. The best optimum position of pigeon i is also employed to update the position of pigeon i in next generation. In addition, the neighborhood of the non-inferior solutions is searched when the suspicious optimum solution meets the search terms. The iteration of the ISMC-PIO is equal to the basic PIO. Therefore, the time complexity of the ISMC-PIO is also $O(N'(N^t \cdot \log N^t + D \cdot N^t + f_{\cos t} \cdot N^t))$.

III. UAV Formation by Optimized RHC Controller

A. The model of UAV

UAVs formation flight is based on the point mass aircraft model in this research. This model can ensure the real-time online solution. The influence of external factors is not taken into account. In this paper, the fuel expenditure is ignored. The leader model without air disturbance is obtained [18]. It is shown in (7).

$$\begin{cases} \dot{x} = -\dfrac{\bar{y}}{\tau_{\psi_W}} \cdot \psi_W - V_W + V_L \cdot \sin\psi_w + \dfrac{\bar{y}}{\tau_{\psi_W}} \cdot \psi_{W_c} \\ \dot{y} = V_L \cdot \sin\psi_W + \dfrac{\bar{x}}{\tau_{\psi_W}} \cdot \psi_W - \dfrac{\bar{x}}{\tau_{\psi_W}} \cdot \psi_{W_c} \\ \dot{z} = \zeta \\ \dot{\zeta} = -(\dfrac{1}{\tau_a} + \dfrac{1}{\tau_b}) \cdot \zeta - \dfrac{z - h_{W_c} + h_{L_c}}{\tau_a \cdot \tau_b} \end{cases} \tag{7}$$

where V_L and V_W are the velocity component in horizontal direction of leader and follower respectively, the yaw angle of leader is expressed by ψ_L, ψ_W denotes the yaw angle of follower, h_{L_c} and h_{W_c} indicate the flight altitude of leader and follower.

Considering the influence of upwash purling of leader [18], the model of follower is as follow.

$$\begin{cases} \dot{x} = -\dfrac{\bar{y}}{\tau_{\psi_W}} \cdot \psi_W - V_W + V_L + \dfrac{\bar{y}}{\tau_{\psi_W}} \cdot \psi_{W_c} \\ \quad + \bar{y}\dfrac{\bar{q}S}{mV}[\Delta C_{Y_{W_y}} y + \Delta C_{Y_{W_z}} z] \\ \dot{y} = (\dfrac{\bar{x}}{\tau_{\psi_W}} - V) \cdot \psi_W + V \cdot \psi_W - \dfrac{\bar{x}}{\tau_{\psi_W}} \cdot \psi_{W_c} \\ \quad - \bar{x}\dfrac{\bar{q}S}{mV}[\Delta C_{Y_{W_y}} y + \Delta C_{Y_{W_z}} z] \\ \dot{z} = \zeta \\ \dot{\zeta} = -(\dfrac{1}{\tau_a} + \dfrac{1}{\tau_b}) \cdot \zeta - \dfrac{z - h_{W_c} + h_{L_c}}{\tau_a \cdot \tau_b} \\ \quad + \dfrac{\bar{q}S}{m}\Delta C_{L_{W_y}} y \\ \dot{\psi}_W = -\dfrac{1}{\tau_{\psi_W}} \cdot \psi_W + \dfrac{1}{\tau_{\psi_W}} \cdot \psi_{W_c} \\ \quad + \bar{x}\dfrac{\bar{q}S}{mV}[\Delta C_{Y_{W_y}} y + \Delta C_{Y_{W_z}} z] \\ \dot{V}_W = -\dfrac{1}{\tau_{V_W}} \cdot V_W + \dfrac{1}{\tau_{V_W}} \cdot V_{W_c} + \dfrac{\bar{q}S}{m}\Delta C_{D_{W_z}} z \end{cases} \tag{8}$$

where $\bar{x}, \bar{y}, \bar{z}$ denote the expected distance between leader and follower in longitudinal, transverse and vertical directions. The dynamic pressure is expressed by $\bar{q}$. S is the wing area. V is the inflow velocity. m shows the mass of the UAV. Assuming that m is unchanged in this research. The resistance coefficient is indicated by $\Delta C_{D_{W_z}}$. $\Delta C_{Y_{W_y}}, \Delta C_{Y_{W_z}}$ are the lateral force coefficient. $\Delta C_{L_{W_y}}$ says the lift coefficient x, y, z are the relative distances in vertical, lateral and elevation direction respectively.

The actual velocity, yaw angle and altitude of leader are said by V_L, ψ_L, h_L respectively. V_W, ψ_W, h_W expresses the actual velocity, heading angle and altitude of follower respectively. $V_{L_c}, \psi_{L_c}, h_{L_c}$ and $V_{W_c}, \psi_{W_c}, h_{W_c}$ are the control inputs of leader and followers. Therefore, $[x, y, V_W, \psi_W, z, \zeta]^T$ is defined as the state variable. $[V_{W_c}, \psi_{W_c}, h_{W_c}]^T$ is regarded as control variables.

As a result, the UAV model (8) can be expressed by

$$\boldsymbol{\dot{X} = AX + BU} \tag{9}$$

where A and B are the coefficient matrix, $\boldsymbol{X} = [x_1, x_2, \cdots x_k, \cdots x_N], k = 1, 2, \cdots, N, \boldsymbol{x}_k = [x, y, V_W, \psi_W, z, \zeta]^T$, where x_k is the state of UAV at k time, $\boldsymbol{U} = [u_1, u_2, \cdots, u_k, \cdots, u_N], k = 1, 2, \cdots, N$, $\boldsymbol{u}_k = [V_{W_c}, \psi_{W_c}, h_{W_c}]^T$, where u_k denotes the control input at k time. The state of UAV at $k+1$ time is predicted by the state at k time. The prediction model is as shown.

$$\boldsymbol{x_{k+1} = Ax_k + Bu_k} \tag{10}$$

where $\boldsymbol{x}_{k+1}$ says the state of UAV at *k+1* time.

B. Equations The model of RHC

RHC is a model based on feedback control strategy. The current state is taken as the initial state at each sampling time. An optimal control problem in finite time domain is solved online based on the state space model and constraints of the system [19]. The first optimum solution is implemented to the system. Then, repeat the above operation. For UAVs formation, RHC is an effective control method. In the formation process, every input is to solve an optimization problem with several constrains in a finite time domain.

To evaluate the solution that is imported into the formation system, a cost function is designed. The cost function is influenced by the system state and control input. The optimized parameters of RHC controller for the formation system are obtained when J_{QP} gains the minimum. Then, the fixed distance among UAVs and the smaller control input can be achieved. The cost function is calculated in a specified time domain after the present moment. Suggest that N is the length of the fixed time interval. Then, the cost function of the RHC controller of the followers [20] is as shown.

$$J_{QP} = \tilde{u}^T (H_u^T \tilde{Q} H_u + \tilde{R})\tilde{u} + 2(H_x x_k - \tilde{x}_{ref})^T \tilde{Q} H_u \tilde{u} \tag{11}$$

where x_k denotes the initial state, the control input is indicated by $\tilde{u}$, the cost function J_{QP} is related to x_k and $\tilde{u}$. R and Q are weighting matrixes. And they are positive definite matrixes. $\tilde{Q} = diag\{Q, \cdots Q\}$, $\tilde{R} = diag\{R, \cdots, R\}$. The predicted system

state is shown by $\tilde{x}_{ref} = (x_{ref,k+1}, x_{ref,k+2}, \cdots, x_{ref,k+i}, \cdots, x_{ref,k+N})^T$. In addition, the state prediction is $\tilde{x} = (x_{k+1|k}, x_{k+2|k}, \cdots x_{k+N|k})^T$, the corresponding control input is described by $\tilde{u} = (u_{k|k}, u_{k+1|k}, \cdots u_{k+N-1|k})^T$. Then, the relationship between $\tilde{x}$ and $\tilde{u}$ is $\tilde{x} = H_x x_k + H_u \tilde{u}$, where $H_x = (A, A^2, \cdots, A^i, \cdots A^N)^T$,

$$\boldsymbol{H}_u = \begin{bmatrix} B & 0 & \cdots & 0 & 0 \\ AB & B & \cdots & \vdots & \vdots \\ \vdots & \vdots & & B & 0 \\ A^{N-1}B & A^{N-2}B & \cdots & AB & B \end{bmatrix}.$$

C. RHC Controller of Formation Flight

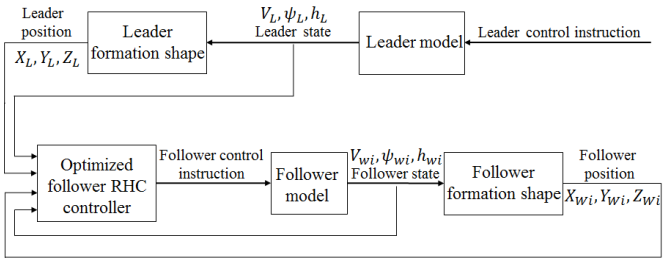

Fig. 3. The structure of RHC controller of UAV formation flight.

Fig.3 shows the structure of RHC for UAV formation based on ISMC-PIO. The input of RHC controller is influenced by the current state of leader, the current position of leader, the feedback on the current state of followers and the feedback on the current position of followers. The follower control instruction is output of the optimized controller based on ISMC-PIO, where *i=2,3,4,5*. The optimized parameters are engine thrust which is in range of [10,100] decided by the throttle, the banking angle that is located from $-\pi$ to π influenced by the ailerons and rudder, and the g-load which is in range of [-5,5] controlled by elevator.

The quadratic programming UAVs formation model is transformed to obtain the minimum of J_{QP}. Based on (9), the velocity channel and heading angle channel are first-order inertial models. The altitude channel is a second-order inertial model. Therefore, the RHC formation controller is implemented in the following steps.

- The state of follower is x_0 at k time. The optimum control input $\tilde{u}^* = [u_1^*, u_2^*, \cdots, u_3^*, \cdots, u_N^*]$ is achieved by solving the optimization problem based on (11). u_1^* is selected as the input of follower RHC. And $u_2^*, \cdots, u_3^*, \cdots, u_N^*$ are ignored.
- Update follower state to a new state x_1 at $k+1$ time.
- Record the state of follower to x_0, and mark the current time to k. Then, go back to the first step and loop again.

With the optimized RHC controller of formation flight, the UAVs would form V-shaped formation from random positions. Followers and the leader take off from different positions. As formation tasks proceed, they flight on the same altitude H with the same velocity in *V*-shape. The formation diagram is shown in Fig.4.

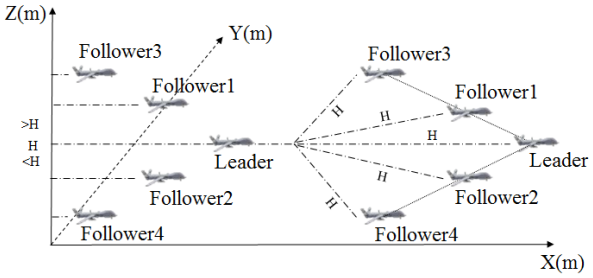

Fig. 4. The formation diagram of UAVs.

IV. Results

Leader-follower method is one of the most commonly used method for UAVs formation control. Leader follows a predefined trajectory. The trajectories of leader and followers maintain a fixed configuration and relative relationship. The velocities of them achieve the same finally. Leader can be regarded as the object of target tracking in this formation style. In this section, the presented ISMC-PIO is employed for the formation flight, and considerable contrast experiments are actualized. Furthermore, outfield experiment are implemented to verify the effectiveness of the proposed ISMC-PIO.

A. Simulation Results

Five UAVs are employed to verify the effectiveness of the proposed RHC for UAVs formation based on ISMC-PIO optimization algorithm, where one is the leader, the other four are the followers. Assume that every mass of the UAV is *1.5Kg*. In addition, three constraints need to be met. The velocities of all UAVs are less than *80m/s*, the engine thrust is among *10N* to *100N*, and the heading angle is among -50° to 50°.

TABLE I. Initial State of UAVs

Parameter	Initial State of UAVs				
	Leader	***Follower1***	***Follower2***	***Follower3***	***Follower4***
$x_i(m)$	0	-600	600	-600	-600
$y_i(N)$	0	300	-300	-600	-600
$z_i(m)$	300	200	100	500	400
$V_L(m/s)$	50	50	50	50	50
$\psi(\circ)$	0	0	0	0	0
$\xi(m/s)$	0	0	0	0	0

The initial state of leader and followers are shown in Table I. The leader is at the front of the formation. It flies with $50\,m/s$ at $300m$ altitude. The followers take off from different positions. Then, they adjust themselves and track the leader and maintain a certain position relationship. In the simulation experiment, the followers fly from different altitudes and positions. As a result, they adjust their attitude to follow the leader at the same altitude based on the proposed method.

TABLE II. INITIAL PARAMETERS OF ISMC-PIOAND OTHERS

Method	Initial Parameters		
	Parameter	***Description***	***Value***
ABC	N	Number of bees	30
	N_F	Number of food bees	$N/2$
	L	Search times	25
	T	Number of generation	100
PIO	N	Number of pigeons	30
	T_1	Number of generation of the map and compass operator	20
	T_2	Number of generation of the landmark operator	10
	R	Influence factor	0.3
PSO	N	Number of particle	30
	T	Number of generation	30
	ω	Inertia factor	0.2
	c_1	Self-learning operator	2
	c_2	Social-learning factor	2
ISMC-PIO	N	Number of pigeons	30
	T_1	Number of generation of the map and compass operator	20
	T_2	Number of generation of the landmark operator	10
	R	Influence factor	0.3
	c	Learning factor	2
	γ	Selected factor	20

To verify the effectiveness and stability of this proposed ISMC-PIO algorithm, four contrast optimization algorithms are implemented to optimize the RHC for UAVs formation, such as the basic PIO, the classical PSO, and ABC etc. The parameters of ABC, basic PIO, PSO and the proposed ISMC-PIO are shown in Table II respectively. The generation number and population size are set to the same. And other parameters of these are confirmed by the existing experience and experiments. Therefore, the results of different method can be compared truly.

Fig.5 shows the cost value contrast curve among PSO, PIO, ABC, ISMC-PIO for UAVs formation. The cost values of them are the average results after 30 simulation results. These four methods can get the their own better cost values. Obviously, the proposed method is better than others. The results in enlarged curve are clear among 60~160 iterations. ISMC-PIO method obtained a better solution at 18 iteration. The convergence rate of PIO is slower than others. In addition, PIO is easy to fall into the local optimum. The effect of PSO is next to ISMC-PIO. ABC is between PIO and PSO. In conclusion, the proposed IMSC-PIO can avoid falling into local optimum and converge to the global optimum rapidly.

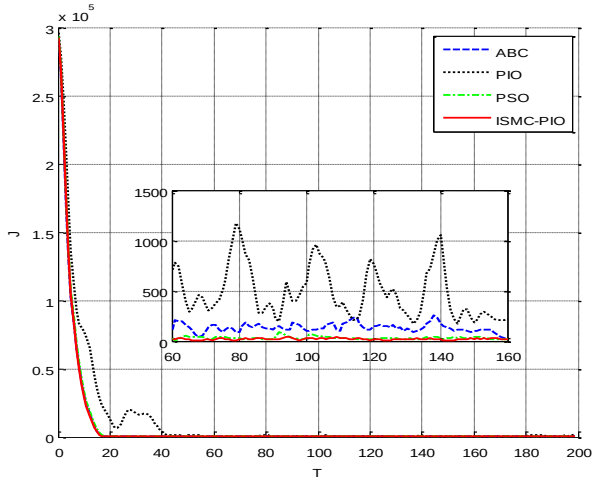

Fig. 5. The cost value contrast curves of ISMC-PIO and others.

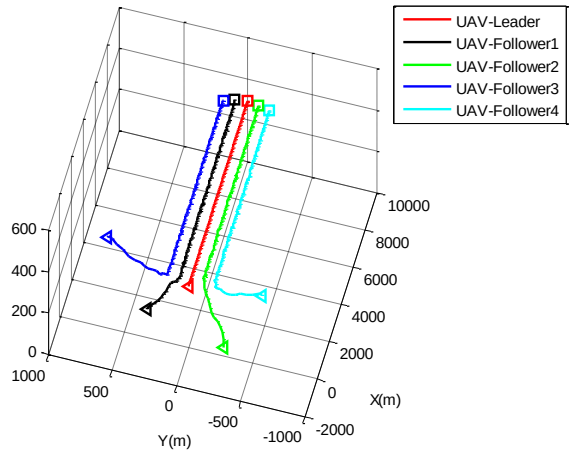

Fig. 6. The formation trajectory of UAVs.

Then, RHC for UAVs formation is implemented by the method ISMC-PIO optimization. The formation result is shown in Fig.6. The "△" is the take-off position of formation. "□" presents the landing position. The leader flies to the $300m$ altitude with 50m/s velocity stably. Follower 1 ~ Follower 4 alter their velocities and altitudes to follow the leader rapidly from different positions. However, the fluctuation is obvious when they are about to stabilize at $300m$. The following tracking is impressive after the fluctuation process. The follow procedures of Follower 3 and Follower 4 are gentle compared with Follower 1 and Follower 2 based on the rule of leader-follower model. Generally speaking, the five UAVs can complete the formation mission.

Fig.7, Fig.8 and Fig.9 express the velocity curves, heading angle curve and pitch angle curve of UAVs in the UAVs formation respectively. The simulation duration is 20 seconds. As shown in Fig.7, the leader flies smoothly with $50\,m/s$. The velocities of Follower 1 ~ Follower 4 change from $37\,m/s$ to $80\,m/s$ before 3 seconds. They are limited in the permissible

range of the above velocity. After completing the initial formation, the velocity of followers change in range of $50 \pm 5 m/s$ after 3 seconds. Followers track the leader state and keep formation within *5m/s* amplitude.

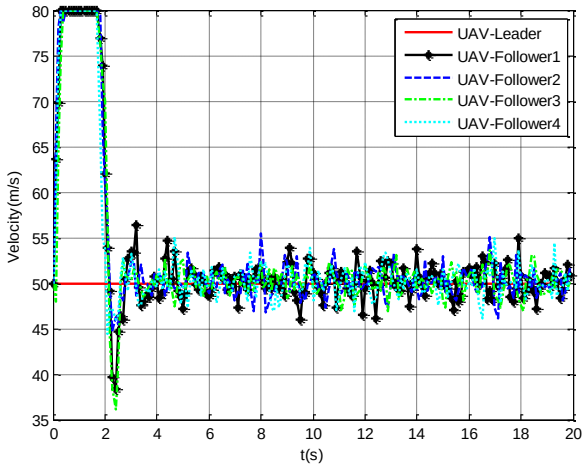

Fig. 7. The velocity curve of UAVs formation.

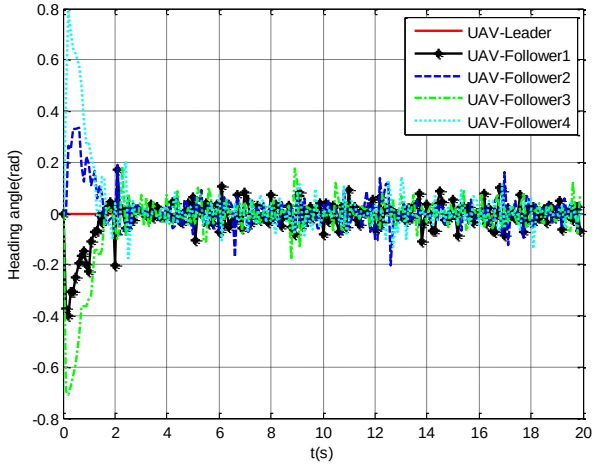

Fig. 8. The heading angle curve of UAVs formation.

Fig.8 shows the leader holds the heading angle at 0*rad* in whole formation. Due to the followers are arranged at different positions, they correct their heading angle to achieve formation mission. Therefore, some larger changes appear before 2 seconds. Then, the heading angle of followers are stable relatively and the change of them are tiny among 2s~20s. The heading angle of follower fluctuate from *-0.2rad* to *0.2rad*.

Same as the above analysis method, the leader keeps a steady 0*rad* pitch angle in the formation flight in Fig.9. The pitch angles of followers vary in range of *-0.4rad ~ 0.49rad* before 2 seconds. Then, followers track the leader within *0.2rad* amplitude and keep formation flight.

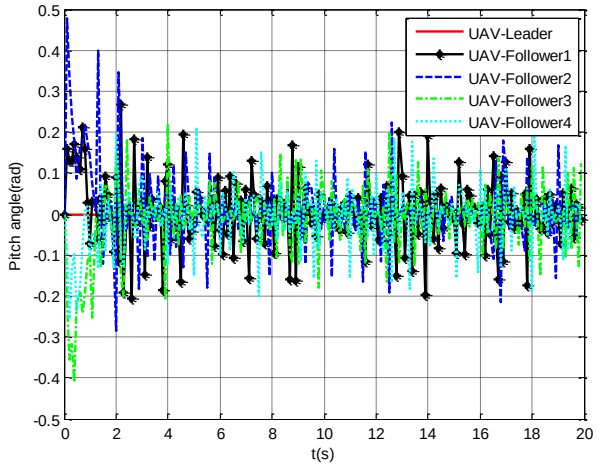

Fig. 9. The pitch angle curve of UAVs formation.

RHC for UAVs formation based on ISMC-PIO optimization in simulation environment has a basic implementation. Within the allowable range of errors, the formation mission is achieved stably and effectively. Follower 1~ Follower 4 can track the leader from different initial positions. The formation mission is accomplished by adjusting the velocities, heading angles and pitch angles of UAVs. To sum up, the proposed ISMC-PIO shows better characteristics in avoiding fall into the local optimum and convergence rate.

B. Outfield Experiment

Some outdoor experiments are implemented to attest the availability of the proposed ISMC-PIO. Due to the limitation of test condition, five quadrotor UAVs are employed to be the formation UAVs.

The mass of each UAV is about *1.5Kg*. They communicate with each other in their own local area network (LAN). Considering the area restrictions and safety issues, the maximum velocity of the UAV is *1.5m/s*. The initial position of UAVs are shown in Fig.10(a). The North East Down (NED) coordinate is shown in the lower-left corner of Fig.11. The formation mission of these five UAVs is that they fly together from north to north with "V" shape. Fig.10(b) shows a moment in the formation process. Followers follow the leader and retain an approximate "V" formation steadily.

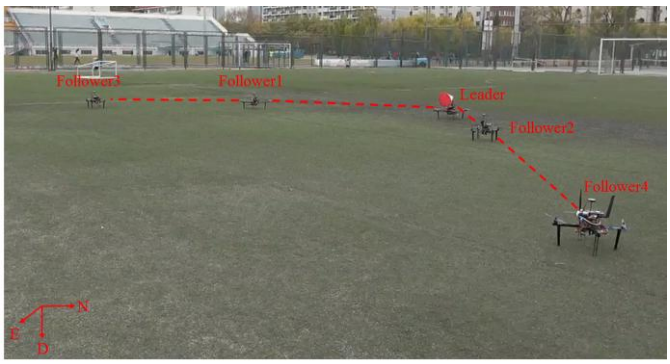

(a) The initial positions of UAVs formation in outdoor.

(b) A moment in formation process.

Fig. 10. The pitch angle curve of UAVs formation.

V. CONCLUSION

A modified pigeon-inspired optimization (PIO) is proposed in this paper. The optimal parameters of receding horizon control (RHC) for UAVs formation is obtained by the presented ISMC-PIO optimization algorithm. Independent search strategy and multi-area convergence mechanism are imported to enhance the ability of global search and avoid falling into the local optimum. Numerous experiments show that the convergence rate and the global searching performance of ISMC-PIO exceeds the basic PIO, PSO and ABC in optimizing the parameters of RHC.

Our future work will concentrate on the considerable outdoor experiments verification. The ISMC-PIO should be used in the quadrotor UAVs robustly [21]. Furthermore, the model of the modified ISMC-PIO will be more perfect. Then, it would be implemented in more complicated parameters optimal problem and application system [22].

REFERENCES

[1] Y. Johnson and S. Dasgupta, "Robust hurwitz stability and performance analysis of H-Infinity controlled forward-velocity dynamics of UAVs in close formation flight using bounded phase conditions in a kharitonov framework," J. of the Institution of Engineers, vol. 95, pp. 223–231, 2014.

[2] X. H. Wang, V. Yadav and S. N. Bala krishnan, "Cooperative UAV Formation Flying With Obstacle/Collision Avoidance," IEEE Trans.on Control System Technology, vol.15, pp.672–679, 2007.

[3] F. Giulietti, L. Pollini and M. Innocenti, "Autonomous formation flight," IEEE Control SYST. Mag., vol. 20, pp. 34–44, 2000.

[4] A. Maqsood and T. H. Go, "Multiple time scale analysis of aircraft longitudinal dynamics with aerodynamic vectoring," Nonlinear Dyn., vol. 69, pp. 731–742, 2012.

[5] B. L Chang, "A dynamic virtual structure formation control for fixed-wing UAVs," IEEE International Conf. on Control and Automation, pp.627–632, Santiago, 2011.

[6] K. A. Ghamry, Y. Dong, M. and A. Kamel, "Real-time autonomous take-off, tracking and landing of UAV on a moving UGV platform," Proceedings of the Mediterranean Conf. on Control and Automation, pp. 1236–1241, 2016.

[7] S. Kim, Y. Kim and A. Tsourdos, "Optimized behavioural UAV formation flight controller design" Proceedings of the European Control Conference, pp. 4973–4978, 2009.

[8] Z. Peng and L. Jikai, "On new UAV flight control system based on Kalman&PID," Proceedings of 2nd International Conf. on Intelligent Control and Information Processing, pp. 819–823, 2011.

[9] J. Shin, S. Kim and J. Suk, "Development of robust flocking control law for multiple UAVs using behavioral decentralized method," J. of the Korean Society for Aeronautical and Space Sciences, vol. 43, pp. 859–867, 2015.

[10] N. H. M. Linorman and H. H. T. Liu, "Formation UAV flight control using virtual structure and motion synchronization," American Control Conf., pp.1782–1787, 2008.

[11] D. Cai, J, Sun and S. T. Wu, "UAVs formation flight control based on behavior and virtual structure," Berlin: Springer, pp. 429–438, 2012.

[12] T. Keviczky, F. Borrelli and G. J. Balas, "Decentralized receding horizon control for large scale dynamically decoupled systems," Automatica, vol. 42, pp. 2105–2115, 2006.

[13] H. B. Duan and S. Q. Liu, "Non-linear dual-mode receding horizon control for multiple unmanned air vehicles formation flight based on chaotic particle swarm optimization," IET Control Theory Appl., vol. 4, pp.2565–2578, 2010.

[14] C. H. Im, H. K. Jung and Y. J. Kim, "Hybrid genetic algorithm for electromagnetic topology optimization," IEEE Trans. Magn., vol. 39, pp. 2163–2169, 2003.

[15] H. Hossein and M. Mardani, "Applying artificial bee colony algorithm for feature optimization in UAV navigation," International J. of Computer and Technology, vol. 15, pp. 2277–3061, 2016.

[16] H. X. Qiu and H. B. Duan, "Receding horizon control for multiple UAV formation flight based on modified brain storm optimization," Nonlinear Dyn., vol.78, pp. 1973–1988, 2014.

[17] H. B. Duan and P. X. Qiao, "Pigeon-inspired optimization: A new swarm intelligence optimizer for air robot path planning," International J. Computer Cybernetics, vol.7, pp.508–511, 2014.

[18] Z. Y. Yang, H. B. Duan and Y. M. Fan, "Unmanned aerial vehicle formation controller design via the behavior mechanism in wild geese based on Levy flight pigeon–inspired optimization," Science China, vol. 48, pp. 161-169, 2018.

[19] W. B. Wang, X. L. Qin, L. G. Zhang and G. H. Zhang, "Dynamic UAV trajectory planning based on receding horizon, " CAAI Trans. On Intelligent Systems, vol. 13, pp. 524–533, 2018.

[20] S. L. Hua, H. You and H. Zhang, "Receding horizon control of UAV formations," Electronics Optics and Control, vol. 19, pp. 1–5, 2012.

[21] H. B. Duan and X. H. Wang, "Echo state networks with orthogonal pigeoninspired optimization for image restoration," IEEE Trans. Neural Netw. Learning Systerm, vol. 27, pp.2413–2425, 2017.

[22] Q. Xue and H. B. Duan, "Robust attitude control for reusable launch vehicles based on fractional calculus and pigeon-inspired optimization," IEEE/CAA J. Automatica Scinica, vol.4, pp.80–97,2017.